ORIGINAL ARTICLE

Evaluating the feasibility of direct contact membrane distillation and nanofiltration in ground water treatment through a techno-economic analysis

Noureddine Elboughdiri[1,2] · Renzun Cosma[3] · Abdelfattah Amari[4] · Velibor Spalevic[5,6] · Branislav Dudic[7,8] · Goran Skataric[9,10]

Abstract

This study delves into the realm of water treatment by conducting a comprehensive techno-economic evaluation of direct contact membrane distillation (DCMD) and nanofiltration (NF) processes. While previous research has explored the technical aspects of membrane distillation (MD) and nanofiltration, there remains a notable gap in economic analyses. Our research aims to bridge this gap by assessing the financial feasibility of employing MD and NF technologies for water desalination. Specifically, we scrutinize the performance of hydrophobic microporous flat sheet membranes crafted from polytetrafluoroethylene (PTFE) supported by non-woven polypropylene (PP) in desalinating brackish water through DCMD and NF processes. By varying operating conditions such as flow rate and feed temperature, we evaluate the membrane's efficacy. Employing an analytical model based on heat and mass transfer equations, we predict process performance across diverse scenarios. Our model demonstrates a high level of accuracy, with flux predictions deviating by less than 10% when utilizing the Knudsen-molecular mechanism model. Furthermore, through a detailed design and economic analysis of industrial-scale units for both processes, we reveal that the cost of permeated water is lower with NF compared to DCMD. Specifically, our calculations indicate a water cost of 1.34 USD/m^3 for DCMD at a feed temperature of 65 °C with an 80% recovery rate, positioning it as a competitive option among conventional desalination methods. Notably, our financial assessment highlights that steam cost constitutes the primary expense in DCMD operations, contingent upon heating value and fuel prices. Noteworthy findings suggest that natural gas emerges as the most cost-effective fuel for steam production in a DCMD plant. This study underscores the economic viability and potential cost efficiencies associated with NF over DCMD in water treatment applications.

Keywords Direct contact membrane distillation (DCMD) · Nanofiltration (NF) · Economic study · Heat and mass transfer

Greek symbols

α_{wf}	Water activity of feed flow
α_{wp}	Water activity of permeate flow
δ_m	Membrane thickness
$\Delta\pi$	Osmotic pressure difference
ε	Membrane porosity
σ_v	Diameter of water vapor collision
σ	Reflection coefficient
τ	Tortuosity

List of symbols

B_m	Knudsen-molecular mass transfer coefficients
d_h	Hydraulic diameter
d_p	Pore size diameter
D_{wa}	Water–air diffusion coefficient
h_f	Heat transfer coefficient of the feed
h_m	Membrane heat transfer coefficient
h_p	Heat transfer coefficient of the permeate
ΔH_v	Enthalpy of vaporization
J_w	Permeate flux
K_n	Knudsen number
k_B	Boltzmann constant
k_f	Thermal conductivities in the feed side
k_p	Thermal conductivities in the permeate side
k_m	Membrane's thermal conductivity
L_p	Membrane permeability coefficient
M_w	Water vapor molecular weight
Nu_f	Nusselt numbers for the feed flow
Nu_p	Nusselt numbers for the permeate flow
P_{mp}	Partial pressure of the permeate flow
P_a	Average air pressure inside the membrane
P_T	Total pressure

Extended author information available on the last page of the article

🙋 Springer

P_m	Average pressure of the pores
P^0_{mp}	The vapor pressures of the permeate surface
P^0_{mf}	The vapor pressures of the feed surface
P_{mf}	Partial pressure of the feed flow
P	Operating pressure
Re	Reynolds number
T_m	Average membrane temperature
T_{bp}	Temperature of permeate bulk
T_{mp}	Temperature of the permeate side membrane
T_{bf}	Temperature of feed bulk
T_{mf}	Temperature of the feed side membrane

Introduction

The rapid growth of the population as well as the expansion of industrial and agricultural activities leads to an increasing need for fresh water. Therefore, one of the most critical global issues is the surge in water demand and the resulting scarcity of water. Although about 97.5% of the surface of the earth is surrounded with water, however just 0.3% of the total fresh water resources are available as fresh water (Hamta and Dehghani 2017; Aydın and Tuna 2018; Ahmed et al. 2019). Groundwater, as a vital natural resource, is a key focus in water treatment due to its importance in meeting the escalating global demand for fresh water. The scarcity of fresh water resources, with only 0.3% of total fresh water available, highlights the urgency to explore innovative methods like desalination to produce fresh water on a large scale. Desalination processes, including membrane distillation (MD) and nanofiltration (NF), have emerged as effective solutions to address water scarcity challenges by purifying brackish water and enhancing water quality. Desalination methods like NF and MD are at the forefront of water purification technologies, offering energy-efficient alternatives to traditional processes like reverse osmosis (RO). MD, a temperature-driven process utilizing vapor pressure differences for separation, stands out for its advantages such as lower operating temperatures and pressures compared to conventional methods like multi-stage flash (MSF) and RO. The direct contact membrane distillation (DCMD) configuration, known for its simplicity and efficiency, is particularly suitable for groundwater desalination due to its ease of operation and maintenance. Consequently, investigations to find new ways to produce fresh water on a large scale has become an important and serious issue all over the world (Zhao et al. 2023). One of these processes, which has recently attracted much attention, is desalination process. Various water treatment and desalination processes can be divided into four categories: pressure-based, concentration-based, temperature-based and electrical-based driving force (Subramani and Jacangelo 2015; Hamta et al. 2017; Tawalbeh et al. 2018; Patel et al. 2020). The temperature-driven

processes such as distillation and evaporation are no longer widely used because of the high energy consumption, various environmental issues and high investment cost (Chen et al. 2021). Other desalination methods are microfiltration (MF) (Jawad et al. 2021), ultrafiltration (UF) (Oré et al. 2022), nanofiltration (NF) (Rosentreter et al. 2021), reverse osmosis (RO) (Stein et al. 2021), electrodialysis (ED) (Generous et al. 2021), reverse electrodialysis (EDR) (Li et al. 2022) as pressure-driven processes and membrane distillation (MD) (Lee et al. 2022) as a temperature-driven process. Two types of the newest water purification methods which have attracted a lot of attention in recent years are NF and MD processes.

Currently, NF—a pressure-driven membrane process—is increasingly being used as a substitute for reverse osmosis in brackish water desalination, owing to its lower energy requirements in comparison with RO (Srivastava et al. 2021). The effective operating parameters in NF membranes, which are capable of removing low molecular weight molecules, are feed temperature, pressure, feed concentration and feed flow rate (Rosentreter et al. 2021; Kukučka and Kukučka Stojanović 2022).

The non-isothermal MD process combines two techniques of distillation and membrane separation. The MD process utilizes difference in vapor pressure as the driving force for separation, with the volatility difference of substances being the key factor in the process. The required difference in vapor pressure between membrane surfaces is achieved through a temperature difference (Luo et al. 2023). A membrane with hydrophobic properties is employed to facilitate the passage of water vapor through the membrane, while the liquid water is rejected, thereby producing water with an exceptionally high level of purity (Anbazhagan et al. 2023). Compared to other conventional desalination processes, the MD has several unique advantages, including lower operating temperature compared to multi-stage flash (MSF) and multi-effect distillation (MED), lower operating pressure compared to RO and also lower heat loss due to the low feed temperature (in the range of 20–80 °C). Fouling is considerably less pronounced in comparison with other membrane-based methods according to its hydrophobic nature and the large pore size of the membrane (Tayefeh 2022). It must be mentioned that the MD is a suitable process for applying sustainable energy options including solar, wind and bioenergy (Elhenawy et al. 2022).

With respect to condensation of vapors occurring on the permeate side, four configurations of MD generally exist: direct contact membrane distillation (DCMD), vacuum membrane distillation (VMD), air gap membrane distillation (AGMD) and sweeping gas membrane distillation (SGMD). Nevertheless, the DCMD has been reported to be the most applicable configuration because of its simplicity in design, operation and maintenance (Yang et al. 2022).

The operational parameters of the MD that effectively influence the process performance are feed properties, and membrane properties such as material, morphology and thickness. Even though the MD process has several advantages compared to usual desalination technologies for the treatment of salty water, the conventional MD membranes have several limitations such as low permeate flux and high thermal polarization (Alqaydi et al. 2022).

As the MD is a temperature-driven process, the heat transfer phenomenon and mass transfer phenomenon must be investigated simultaneously. Generally, the MD mass transfer is occurring because of the condensation of vapors on the permeate side as a result of vapor diffusion through the pores of the membrane. Extensive studies have been already performed on the vapor diffusion in the pores of hydrophobic membranes (Subramanian et al. 2019). In this way, different types of theoretical models for the prediction of vapor flux are available. The dusty model is a commonly employed framework for characterizing mass transfer in MD. This model comprises several mechanisms, namely molecular and surface diffusion, viscous flow and Knudsen diffusion. Bouchrit et al. (2015) studied the MD process to purify brackish water and investigated the Knudsen, molecular and Knudsen-molecular mass transfer models to predict the performance of MD (Bouchrit et al. 2015). According to their published results, the Knudsen-molecular mass transfer model is in acceptable agreement with the obtained data. Ismail et al. (2022) proposed a numerical model with two dimensions to simulate a DCMD module, and the study discovered that the vapor's transmembrane flux can be estimated using Fick's law, and the water flux is hardly influenced by the pressure differential across the membrane's two sides (Ismail et al. 2022). Shirzadi et al. (2022) described the performance of the ammonia in water separation and the transport phenomena of the VMD process by developing a CFD model (Shirzadi et al. 2022).

Since a few economic studies have been conducted on membrane distillation and there is no deep understanding in this regard, after a technical assessment, economic evaluation is necessary to the MD technology implementation (Usman et al. 2021). Thus, in order to assess the economic viability of the MD technique, a techno-economic investigation has been conducted to evaluate its potential for water purification. To estimate the total investment cost, the membrane process financial evaluation was studied by calculating the capital cost (CAPEX) and operating costs (OPEX), and finally the cost modeling was applied (Nthunya et al. 2022).

So far, many studies have been conducted on MD and NF processes, separately; nevertheless, no comprehensive study has been carried out to compare these two processes from the economic and process point of view (Halder et al. 2024). The work aims to study the economic evaluation and the feasibility study of the DCMD and the NF processes in the

desalination of the groundwater. These two desalination processes were chosen to improve the quality of specific underground water. After analyzing the impact of various factors on the efficacy of both procedures, the MD process was scrutinized with regard to feed temperature and the flow rate, while the NF process was evaluated based on feed pressure and feed flow rate. Then, using the results, two processes were scaled up and evaluated according to the existing economic methods. Finally, two processes were compared with each other in terms of performance and economy. Due to the consumed energy price and the heating value on the total cost of the process, it was appropriately discussed economically. In this way, the performance of DCMD and NF using a commercial polytetrafluoroethylene membrane is investigated, and the most critical variables are studied including feed temperature and feed flow rate. Then a predictive model is developed by concurrently solving the heat transfer and mass transfer models.

The novelty of this work lies in its comprehensive techno-economic evaluation of DCMD and NF processes for water treatment. Unlike previous studies that have primarily focused on the technical aspects of these processes, our research bridges the gap by assessing the financial feasibility of employing DCMD and NF technologies for water desalination. By scrutinizing the performance of hydrophobic microporous flat sheet membranes in desalinating brackish water through DCMD and NF processes, we offer a unique perspective on the practical application of these technologies. Additionally, our use of an analytical model based on heat and mass transfer equations to predict process performance across diverse scenarios adds a novel dimension to our study. The model's high level of accuracy in flux predictions, coupled with our detailed comparison of the cost of permeated water between DCMD and NF processes, highlights the cost efficiencies associated with NF over DCMD in water treatment applications. These novel contributions make our research a valuable addition to the existing body of knowledge in the field of water treatment, providing insights that can inform decision-making in the industry.

Materials and methods

Membrane process

Qingfeng Filter Equipment Material Co., Ltd. provided a commercially available flat-sheet membrane composed of polytetrafluoroethylene (PTFE) and supported by a non-woven polypropylene (PP). The membrane specifications include a pore size of 0.45 μm, porosity of 75% and a contact angle of 115 degrees.

Polytetrafluoroethylene membranes are known for their high porosity and surface-to-surface dust-removal

performance, ensuring stable pressure maintenance. PTFE is widely recognized for its excellent physico-chemical properties and is commonly used in various applications, including air filtration systems. The non-woven polypropylene (PP) support provides additional structural integrity to the membrane.

The membrane's pore size of 0.45 μm ensures efficient filtration capabilities, while the high porosity of 75% enhances the performance. Additionally, the contact angle of 115 degrees indicates the membrane's hydrophobic nature, making it suitable for applications requiring water resistance. Overall, the membrane's composition of PTFE and non-woven PP, along with its specific characteristics, makes it a promising material for filtration applications due to its durability, porosity and hydrophobic properties. The brackish groundwater was collected and was used without any pretreatment as the feed. The features of the feed are presented in Table 1.

A schematic representation of the experimental setup for NF is presented in Fig. 1, which illustrates the use of a gauge to record the output pressure of the module. A ball valve is also included in the return flow path to regulate the Reynolds number. Additionally, the flow rate is measured applying a flow meter. During the process, the permeate flux is determined with the help of a digital scale that has an accuracy of ± 0.001 g. Furthermore, a Hypro model roller pump is applied to provide the required pressure of the process. In order to control the feed pressure, a PID controller is used, which operates by adjusting the pump electric motor.

To perform the NF process, first, the desired membrane was subjected to compression using deionized water for 2 h under the operating conditions in terms of pressure and feed flow rate, which should be carried out to prevent undesirable changes in the membrane hydraulic resistance through the process. Then, the desired feed is pumped to the membrane module, where the applied pressure and feed flow rate are adjustable using a controller and a control valve, respectively.

Figure 2 shows a DCMD experimental setup schematic diagram that consisted of feed and permeate loops which is connected to a module. The feed was warmed through a heat exchanger in a feed tank before transport to the module. The permeate flow was cooled to 20 °C in permeate tank using a chiller. The hydrophobic membrane with active membrane

Table 1 The features of the brackish groundwater as the water source

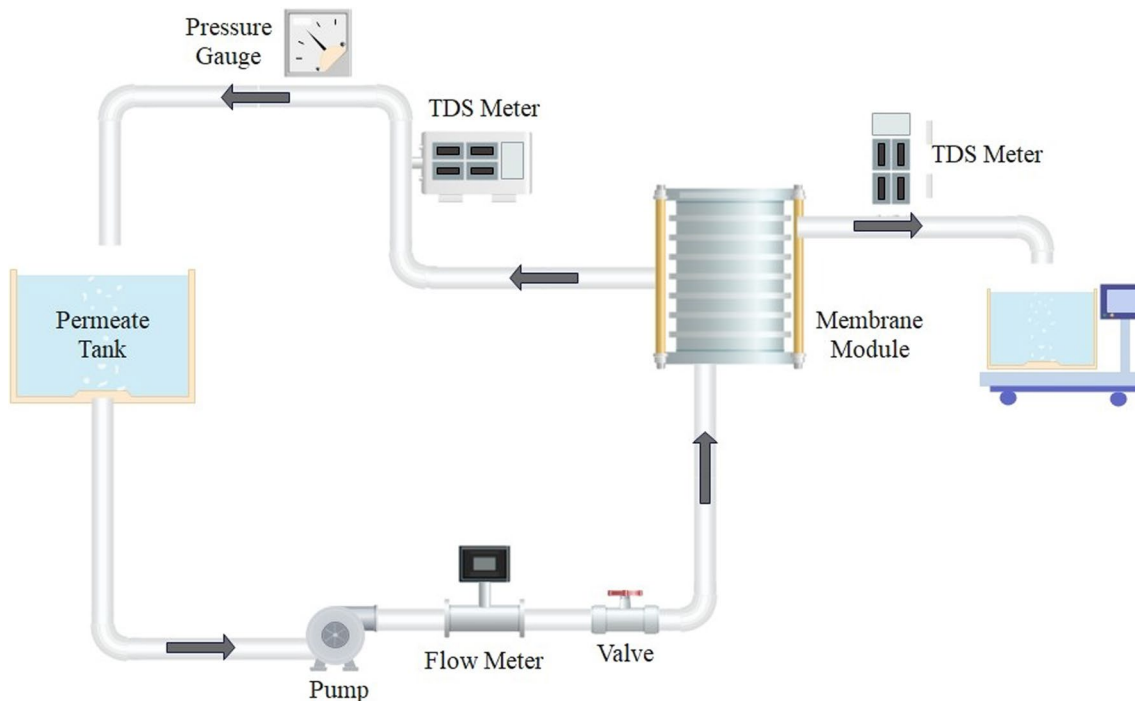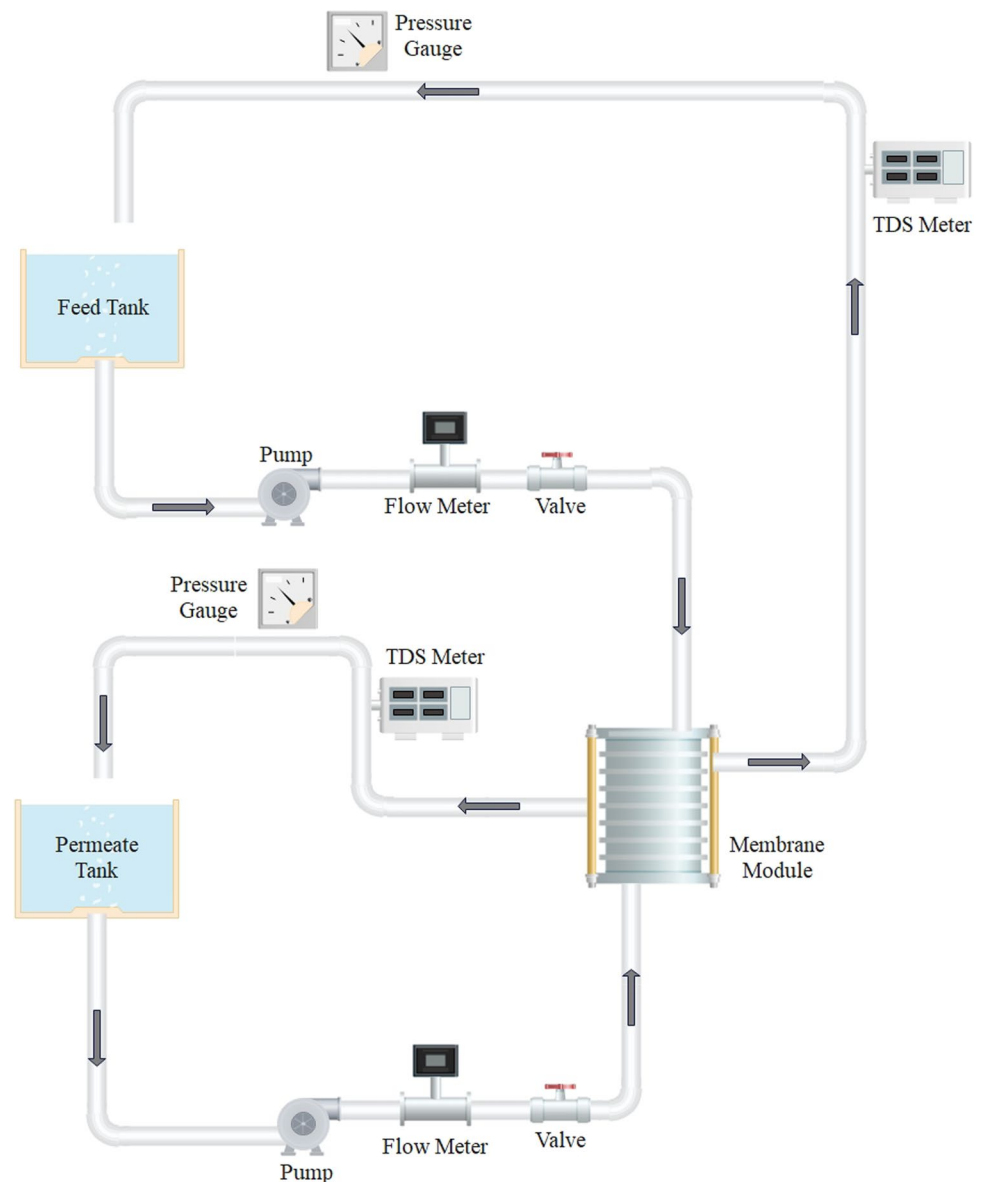| Conductivity (μS/cm)	7150
pH	8.3
Ca^{2+} (mg/L)	220
Na^+ (mg/L)	675
Mg^{2+} (mg/L)	425
K^+ (mg/L)	2.97
Cl^- (mg/L)	1830
SO_4^{2-} (mg/L)	234.9
TDS (mg/L)	4505

Fig. 1 Schematic diagram of NF experimental setup

Fig. 2 Schematic diagram of DCMD experimental setup

area of 32 cm^2 was fixed in the module. A flow control valve was applied to adjust the feed flow into the module using a flow meter for accurate adjustment. The pressure and the temperature of the flows were measured using a manometer and a thermocouple, respectively. The permeate flow was weighed in a permeate reservoir by applying a digital weight balance with an accuracy of ± 0.001 g to calculate the permeate flux.

The data were conducted under various operation conditions, and to study the process performance the flux and rejection were monitored in each experiment. It must be mentioned that the rejection value was calculated using an Electrical Conductivity Meter (EC meter, Emcee Electronics Inc, model 1152, USA). The experiments were performed at different feed flow rates (from 1 LPM to 2.5 LPM with an interval of 0.5 LPM) with the feed temperature varying from 35 to 65 °C with an interval of 10 °C (totally 16 experimental runs). In all the experiments, the temperature was 24oC and the feed flow rate on the cold side was 1.3 LPM.

Heat and mass transfer modeling

One of the most challenging characteristics of MD is the simultaneous operations of heat transfer and mass transfer between the permeate and feed sides. On the other hand, to prognosticate the flux of permeate and interfacial membrane temperature from the MD models, perception of the heat and the mass transfer is essential. To investigate the mass transfer rate in the MD method, the pressure differential of the vapor on either side of the membrane is required. To calculate the vapor pressure, the mean temperature at the interface of the

fabricated membrane can be used, which is calculated from the bulk temperature.

Generally, there are three regions, which heat transfer occurs in a specific flux. In the feed region, heat is convectively transferred from the bulk to the surface of the membrane through the boundary layer. The second region is inside the membrane where heat transfer occurs by two ways; the first way is across the membrane by conduction, and the second mechanism pertains to the diffusion of vapor via the pores that the first one is kind of sensible heat and the second one is latent heat. And the third, convective heat transfer which occurs from the boundary layer to the permeate solution bulk. These three regions are as follows (Santos et al. 2021):

(a) On the feed membrane side, the mechanism of heat transfer is described by Eq. (1)

$$Q_f = h_f(T_{bf} - T_{mf}) \tag{1}$$

where h_f represents the feed heat transfer coefficient and T_{mf} and T_{bf} are the membrane surface and bulk temperature in the feed side, respectively.

(b) As mentioned above, in the membrane matrix, there are generally two forms of mechanisms of heat transfer, including heat transfer by conduction and heat transfer by evaporation mass flux, which are expressed in Eq. (2).

$$Q_m = h_m(T_{mf} - T_{mp}) + J_w \times \Delta H_v \tag{2}$$

where T_{mf} and T_{mp} represent the temperature of the membrane on the feed and permeate, respectively. Furthermore, ΔH_v, h_m and J_w are the enthalpy of vaporization, the membrane heat transfer coefficient and the permeate flux, respectively. The H_v and the h_m can be represented by Eqs. (3) and (4), respectively, where T_{mf} is the temperature of the surface of the membrane at the feed side.

$$H_v = 1.7535 \times T_{mf} + 2024.3 \tag{3}$$

$$h_m = \frac{k_m}{\delta} \tag{4}$$

The variables k_m and δ correspond to the membrane's thermal conductivity and thickness, respectively. Generally, k_m is estimated by two models, as below:

$$k_m = (1 - \varepsilon)k_{mm} + \varepsilon k_g \tag{5}$$

$$k_m = \left[\frac{1 - \varepsilon}{k_g} + \frac{\varepsilon}{k_{mm}}\right]^{-1} \tag{6}$$

where ε, k_g and k_{mm} are the membrane porosity, thermal conductivity of water vapor in the membrane pores and thermal conductivity, respectively.

(c) On the permeate side, the mechanism of heat transfer is described by Eq. (7).

$$Q_P = h_p(T_{mp} - T_{bp}) \tag{7}$$

where h_p represents heat transfer coefficient of permeate. T_{bp} and T_{mp} are the temperature of the permeate bulk and temperature of the permeate side surface of the membrane, respectively. It is obvious that at the steady-state condition we can write:

$$Q_f = Q_m = Q_p \tag{8}$$

The temperature of the surface of the membrane on both, the permeate and the feed sides, in the DCMD module can be calculated using energy balance in Eq. (8). Finally, Eqs. (9) and (10) are iteratively used to predict the temperature of two sides of the membrane surface (Manawi et al. 2014).

$$T_{mf} = \frac{h_m\left(T_{bp} + \left(\frac{h_f}{h_p}\right)T_{bf}\right) + h_f T_{bf} - J_w \Delta H_V}{h_m\left(1 + \frac{h_f}{h_p}\right) + h_f} \tag{9}$$

$$T_{mp} = \frac{h_m\left(T_{bf} + \left(\frac{h_f}{h_p}\right)\right) + h_p T_{bp} + J_w \Delta H_v}{h_m\left(1 + \frac{h_p}{h_f}\right) + h_p} \tag{10}$$

The heat transfer coefficient of the feed (h_f) and the permeate sides (h_p) can be presented by Eqs. (11) and (12), respectively.

$$h_f = \frac{\text{Nu}_f k_f}{d_h} \tag{11}$$

$$h_p = \frac{\text{Nu}_p k_p}{d_h} \tag{12}$$

where k_f and k_p represent the thermal conductivities in the permeate and feed sides, respectively. Nu_f and Nu_p are Nusselt numbers for the feed flow and the permeate stream, respectively, and d_h is the hydraulic diameter.

Many equations are already presented for calculation of Nusselt number of laminar and turbulent flows, which have been reported in extensive studies (Meyer et al. 2019; Guo et al. 2021).

In this work, Eqs. (13) and (14) were applied to calculate the Nusselt number of laminar and turbulent flow (Chen et al. 2017), where Re presents the Reynolds number and Pr is the Prandtl number.

$$\text{Nu}_{f,p} = 1.62(Re_{f,p}Pr_{f,p}(d_h/L))^{\frac{1}{3}}, \text{Re} < 2300 \tag{13}$$

$$\text{Nu}_{f,p} = 0.023\text{Re}_{f,p}^{0.8}\underset{f,p}{\text{Pr}^{\frac{1}{3}}}, \text{Re} > 2300 \tag{14}$$

In a nutshell, to have a prediction for the heat transfer and mass transfer, first of all, the physical properties of the membrane, the morphological membrane parameters, the module geometry and the DCMD operating conditions were defined (König 2023). Since surface temperature measurement of the membrane is not possible, the membrane surface temperature was predicted using the heat transfer method. Then, an iterative method was performed to solve the heat transfer and mass transfer equations simultaneously to measure the permeate flux. As an initial guess, the temperature of the permeate and feed sides were considered equal to the temperature of the bulk of the feed flow and the permeate side, respectively. It must be mentioned that the heat transfer coefficients of laminar and turbulent flows were predicted by Eqs. (13) and (14).

The mass transfer in the DCMD method can be categorized into three areas, which are analogous to heat transfer. The first mechanism involves mass transfer within the feed boundary layer. The second area is via the membrane itself, and the final area is in the permeate boundary layer (Mahmood et al. 2023). Darcy's law is utilized to demonstrate how mass is transported through the hydrophobic membrane's porous structure by Eq. (15).

$$J = B_m(P_{mf} - P_{mp}) \tag{15}$$

where P_{mf}, P_{mp} and B_m are the partial pressure of the feed flow and the permeate side and the membrane distillation coefficient, respectively. The P_{mf} and the P_{mp} can be calculated as follows:

$$P_{mf} = \alpha_{wf}P_{wf}^0 \tag{16}$$

$$P_{mp} = \alpha_{wp}P_{wp}^0 \tag{17}$$

where α_{wf} and α_{wp} are the water activity of feed flow and permeate side and P^0_{mf} and P^0_{mp} are the vapor pressures of the feed surface and the permeate surface, respectively. The $\alpha_{wf,p}$ is given by Eq. (18), where xi is the mole fraction of i in the solution.

$$\alpha_{wf,p} = 1 - x_i - 10x_i^2 \tag{18}$$

The interrelation of mass and heat transfer during the MD process is established through the use of the Antoine equation, which calculates the pressure of vapor at varying temperatures as follows:

$$P_w^0 = \exp\left((23.1964) - \frac{3816.44}{T_m - 46.13}\right) \tag{19}$$

where P_w^0 represents the pressure of water vapor that can be applied on both the feed stream and the permeate side. The boundary layer mass transfer was analyzed using the film theory (Curcio and Drioli 2005) and the dusty-gas model (Lawson and Lloyd 1996), respectively. As was mentioned, molecular diffusion, Knudsen diffusion, as well as surface diffusion and viscous flow are some of the mechanisms of the mass transfer that are included in the dusty model. In order to simplify the model, in DCMD applications, viscous flow and surface diffusion can be disregarded, without significant effect on the correlation. The Knudsen number (K_n) can be exploited to identify the primary mass transport mechanism through the pores of the membrane in DCMD as below:

$$K_n = \frac{\lambda}{d_p} \tag{20}$$

$$\lambda = \frac{k_B T_m}{\sqrt{2}\pi P_m \sigma_v^2} \tag{21}$$

where k_B is Boltzmann constant, T_m is average temperature, σ_v (0.2641 nm) is the diameter of water vapor collision, and P_m is average pressure of the pores.

Briefly, there are three different scenarios: (i) if $K_n > 1$, Knudsen diffusion is dominant, (ii) if $K_n < 0.01$, molecular diffusion is dominant, and (iii) Knudsen-molecular transition when $0.01 < K_n < 1$.

In this work, the Knudsen-molecular mass transfer coefficient (B_m) was calculated as Eq. (22), where τ, δ_m, P_a, T_m, ε, P_T, D_{wa}, d_p and M_w are tortuosity, membrane thickness, average pressure of air inside the membrane, average membrane temperature, membrane porosity, total pressure, water–air diffusion coefficient, pore size diameter and water vapor molecular weight, respectively.

$$B_m = \frac{1}{\frac{3\tau\delta_m}{\varepsilon d_p}\sqrt{\frac{\pi R T_m}{8M_w}} + \frac{\tau\delta_m P_a R T_m}{\varepsilon P_T D_{wa} M_w}} \tag{22}$$

The tortuosity (τ) can be estimated from Eq. (23):

$$\tau = \frac{(2-\varepsilon)^2}{\varepsilon} \tag{23}$$

The product of P_T and D_{wa} for water–air can be expressed in Pa m^{-2} s^{-1} and can be defined as Eq. (24).

$$P_T D_{wa} = 1.895 \times 10^{-5} T_m^{2.072} \tag{24}$$

The calculation flowchart of the heat transfer phenomena and the mass transfer is presented in Fig. 3.
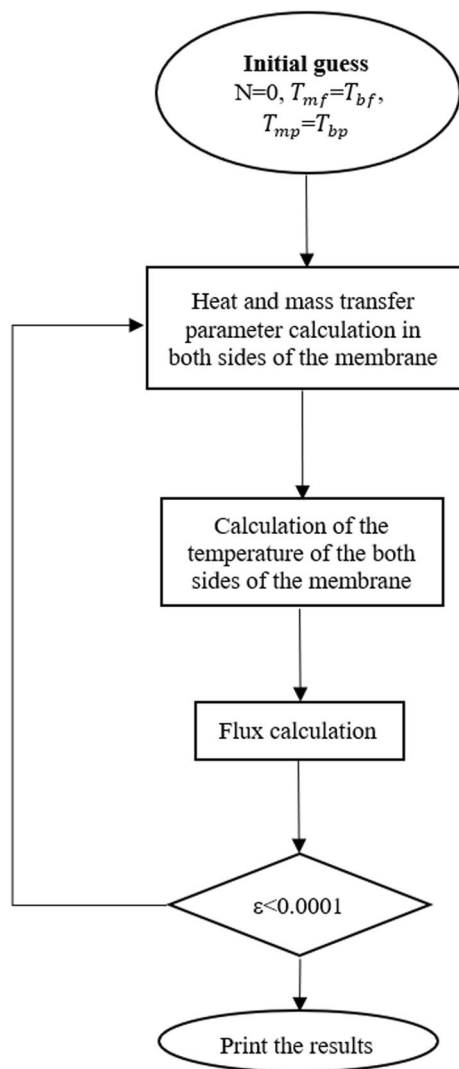
Fig. 3 The calculation flowchart of the heat transfer phenomena and the mass transfer

Results and discussion

NF performance

The features of the nanofiltration process permeate water are given in Table 2. By comparing the results of Table 2 with characteristics of the brackish groundwater (Table 1), it can be concluded that the conductivity is reduced to 4120 from 7150 μS/cm.

As the pressure plays an essential role in the nanofiltration process, the pilot NF tests were conducted at three different pressure levels. An analysis was carried out to examine how the operational pressure impacts the flux of the permeate during the process of nanofiltration, at three pressure levels of 4, 6 and 8 bar. Figure 4 depicts the influence of operating pressure on the permeate flux. As can be seen, the flux of

Table 2 The analysis of the nanofiltration process permeate water

Parameter	Unit	Value
Conductivity	s/cmμ	4120
pH	–	7.1
Ca	ppm	40
Mg	ppm	48.5
Cl	ppm	1119
SO$_4$	ppm	59.9
Na	ppm	12.1
K	ppm	2.63
TDS	ppm	2090

the permeate increases with raising the pressure. It is noteworthy that although the flux of the permeate increases significantly, this increase in pressure causes more compression of the formation of the layer of cake on the surface of the membrane and increases the rate of fouling.

As a result of the feed's low concentration, the flux of the permeate drop-off is less noticeable. Nevertheless, due to membrane fouling, the flux reaches a constant value, which depends on the pressure of the permeate flow. Generally, in pressure-based membrane separation systems, the operating pressure has a positive influence on the permeate; in fact, with increasing the pressure, the flux of the permeate increases, which can be presented as follows.

$$J_v = L_p(\Delta P - \sigma.\Delta\pi) \tag{25}$$

where, L_p, P, σ and $\Delta\pi$ are membrane permeability coefficient, operating pressure, reflection coefficient and osmotic pressure difference, respectively. As can be understood from Eq. (25), as the operating pressure raises, the flux of the permeate raises. Nevertheless, increasing the osmotic pressure has a negative effect on the flow rate. The osmotic pressure has a direct correlation with the concentration of the feed, as the osmotic pressure increases, the flow rate decreases.

The impact of pressure on the permeate TDS in the NF process can be observed in Fig. 5. The results show that the increase in pressure improves the quality of the product water in terms of the TDS.

To explore how the rate of the feed flow affect the flux of the permeate, various flow rates were tested, and the permeate flux values were recorded and are displayed in Fig. 6. The results indicate that an elevated flow rate results in a higher mass transfer coefficient within the concentration polarization layer, as well as in the mixing near the surface of the obtained membrane. This is due to the reduction of the gel layer formed on the membrane surface and the decrease in resistance of the mass transfer. Therefore, the species that accumulate on the surface return to the bulk flow, leading to a raise in the flux of the permeate. It should be mentioned that increasing the flow rate

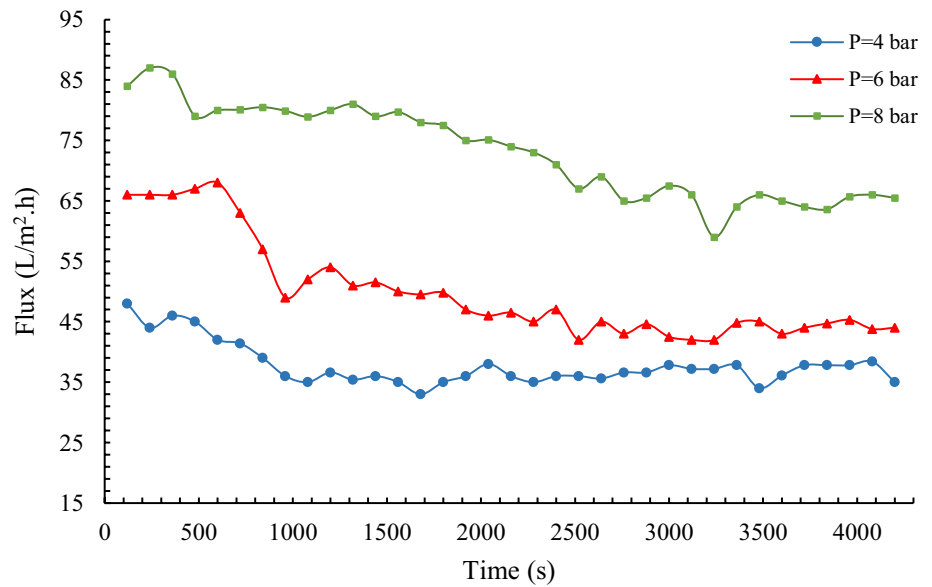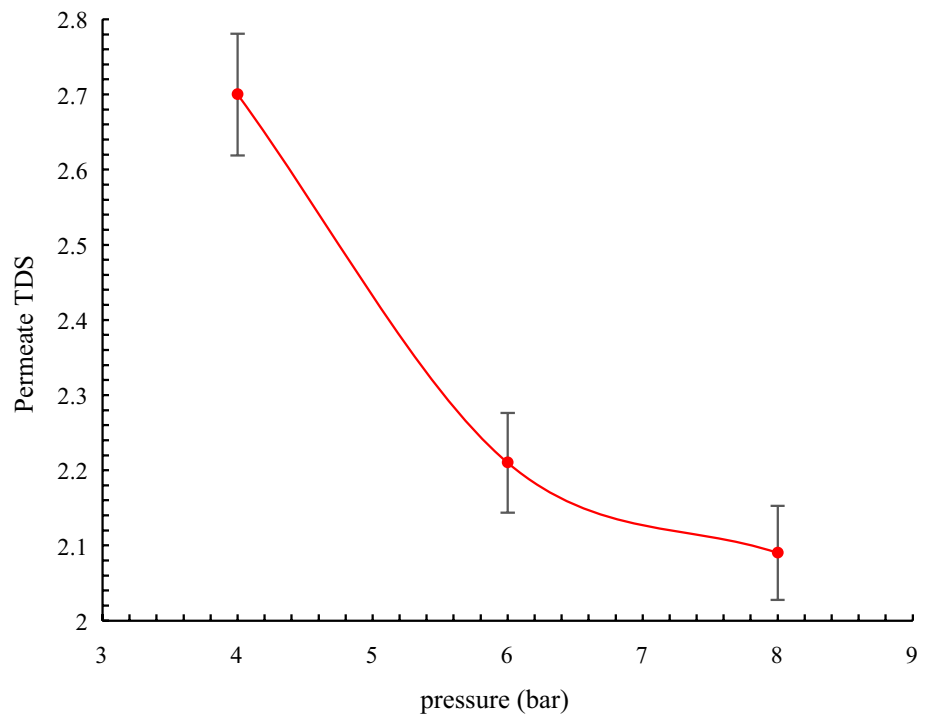**Fig. 4** The nanofiltration membrane permeate flux at different pressures

Fig. 5 The pressure affect on the TDS of the permeate in NF process

requires more energy consumption, so choosing a higher flow rate is not economically desirable. But as can be seen in Fig. 6, raising the rate of the feed flow resulted in a minor raise in the flow rate of the permeate for the process. This outcome can be attributed to the low concentration of the feed, which resulted in the creation of a negligible amount of cake layer on the membrane surface.

DCMD performance

The DCMD process was also investigated to improve the condition of the permeated water. In this way, the DCMD permeate water was analyzed and the results are reported in Table 3. According to experimentally obtained data, it was found that the DCMD permeate water is not suitable for drinking and agricultural uses, due to the very low

Fig. 6 The flux of the permeate of the nanofiltration process at different feed flow rates
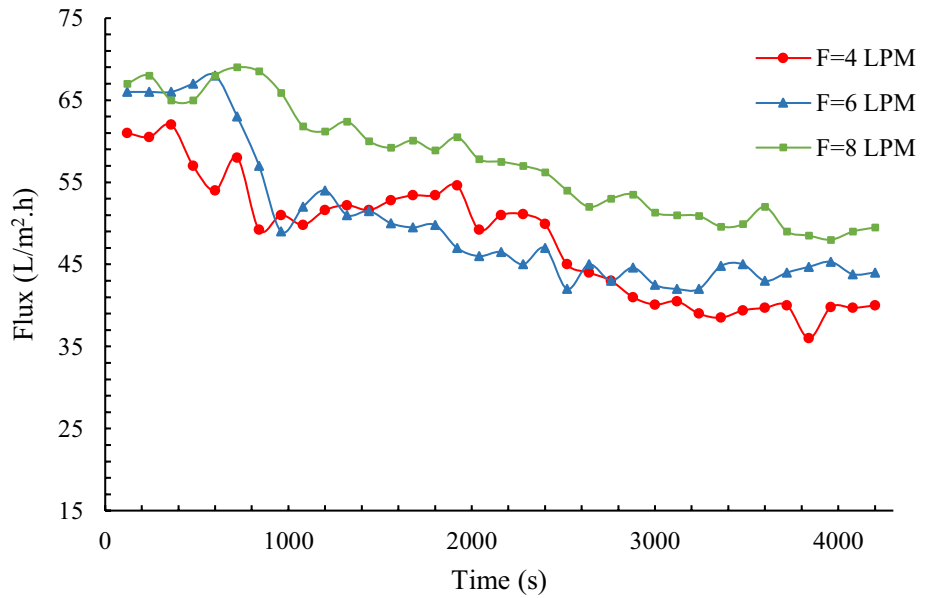
Table 3 The analysis of the DCMD process permeate water

Parameter	Unit	Value
Conductivity	μs/cm	25
pH	–	6.1
Ca	ppm	3.2
Mg	ppm	1.9
Cl	ppm	9.9
SO_4	ppm	2.7
Na	ppm	0.3
K	ppm	0.1
TDS	ppm	18

conductivity (25 μs/cm); nevertheless, it is more suitable for industrial applications that require pure water.

The temperature gap between the feed stream and permeate flow is recognized as the most significant factor that impacts permeate flux in the DCMD method. However, the increase in temperature has limitations in terms of economics and membrane resistance, so that at high temperatures there is a possibility of destroying the membrane structure, or with an increase in temperature, the process may not be economically justified in terms of energy consumption. The temperature effects of the feed on the resulted flux in the DCMD of the permeate are depicted in Fig. 7. As can be understood from Fig. 7, the flux of the permeate has increased significantly with raising the temperature of feed

Fig. 7 The temperature of the feed stream effects on the DCMD permeate flux
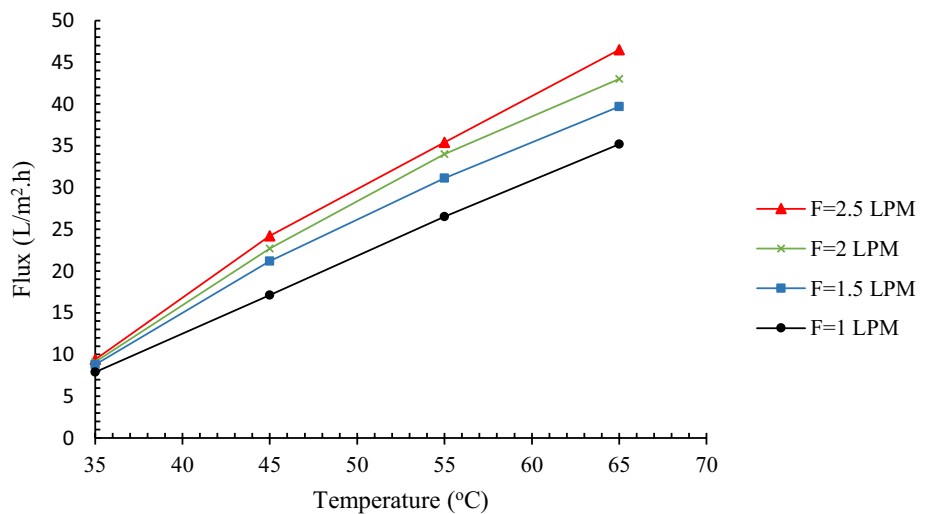
and can be attributed to the notable rise in steam pressure. According to the findings, elevating the temperature of the feed from 35 to 65 °C results in a rise in the flux of the permeate from 7.88 to 35.2 L/m2 h when the flow rate of the feed is set at 1 LPM.

Based on Fig. 7, it is evident that at a feed flow rate of 2.5 LPM increasing the temperature of the feed stream from 35 to 65 °C results in a 395% rise in permeate flux. For feed flow rates of 1 LPM, 1.5 LPM and 2 LPM; the permeate flux increases by approximately 340, 353 and 370%, respectively. The results proved that at higher temperatures of the feed, an increase in the feed flow rate could be more potent to improve the total flux.

In order to have a comparison between the experimental results and the correlated data, the correlation was done at a flow rate of the feed of 1 LPM at different temperatures. The comparison of experimental and theoretical data is demonstrated in Fig. 8. Comparing the obtained data and the theoretical results, shows that the correlation error is less than 3%, which shows that the data prediction is quite reasonable and can be used in different operating conditions.

Figure 9 shows the temperatures effects on the permeate TDS at different temperature difference from 35 to 65 °C using DCMD method. As it is depicted in Fig. 9, the amount of TDS has decreased slightly with the increase in feed temperature.

Experiments were conducted at various flow rates of the feed to examine their impact on permeate flux. As depicted in Fig. 10, increasing the feed flow rate leads to a corresponding raise in flux of the permeate. For instance, elevating the feed flow rate from 1 LPM to 2.5 LPM at a temperature of 65 °C results in a raise in flux of the permeate from
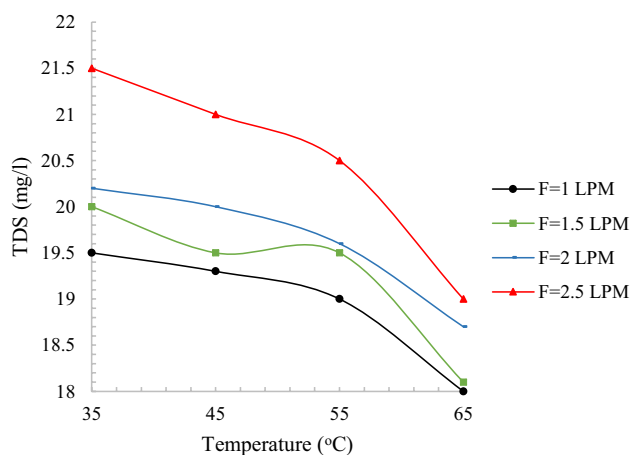

Fig. 9 The temperatures effects on the permeate TDS at different temperature difference from 35 to 65 °C using DCMD process

2.35 to 5.46 L/m^2 h. A similar investigation carried out at feed temperatures of 35, 45, 55 °C demonstrates a 28% raise in flux, which attributed to the rise in flow Reynolds number. As the rate of the feed and flow raises, the Reynolds number increases, leading to turbulent flow and a raise in the mass transfer coefficient within the membrane solution. Additionally, a raise in the Reynolds number can reduce resistance of the transfer of the mass and mitigate the effects of concentration and temperature polarization.

Considering the temperature variance across the permeate and feed stream sides is the primary operational parameter influencing permeate flux in DCMD, the impact of feed temperature on permeate flux was tested by changing the feed temperature from 35 to 65 °C in 10 °C increments. The

Fig. 8 Comparison of experimental and modeling results in the membrane distillation process with feed flow rate of 1 LPM
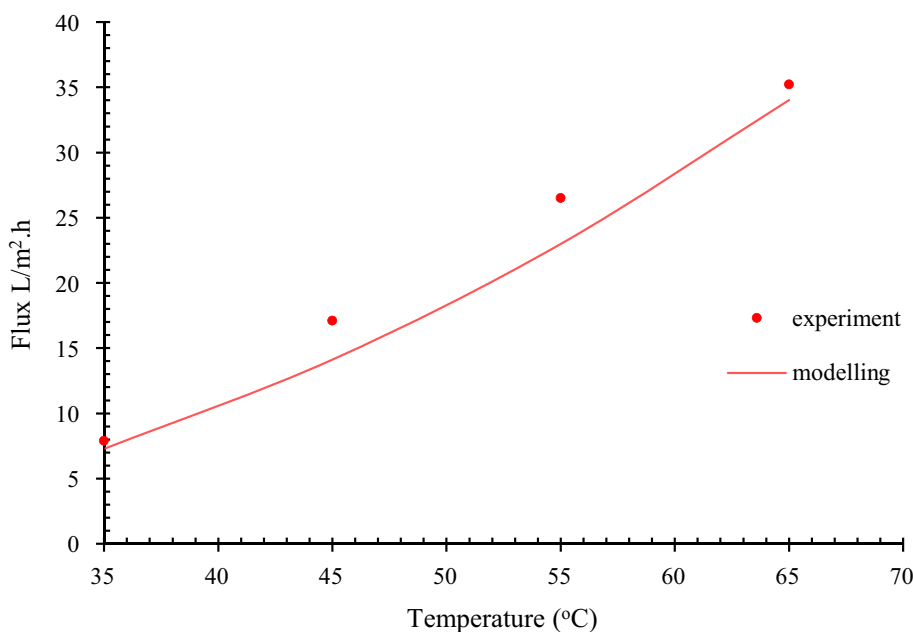
Fig. 10 The permeate flux of the DCMD method at different flow rates of the feed and different temperatures
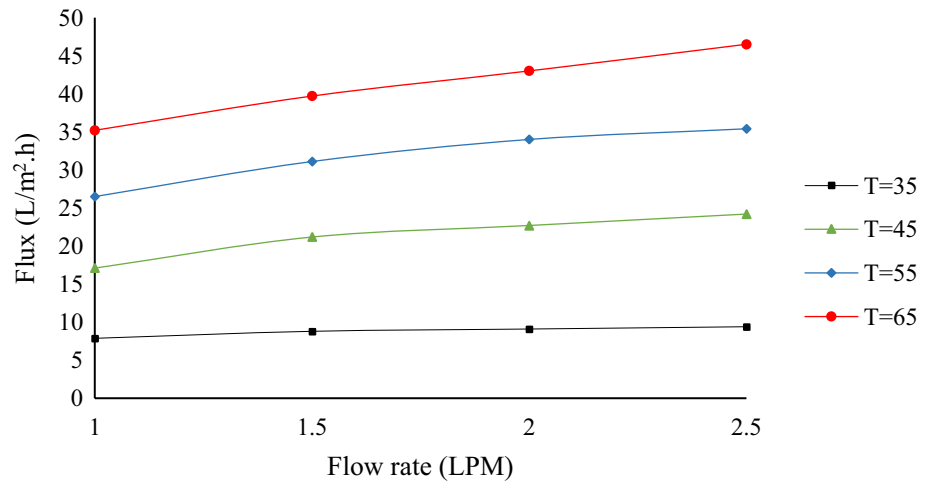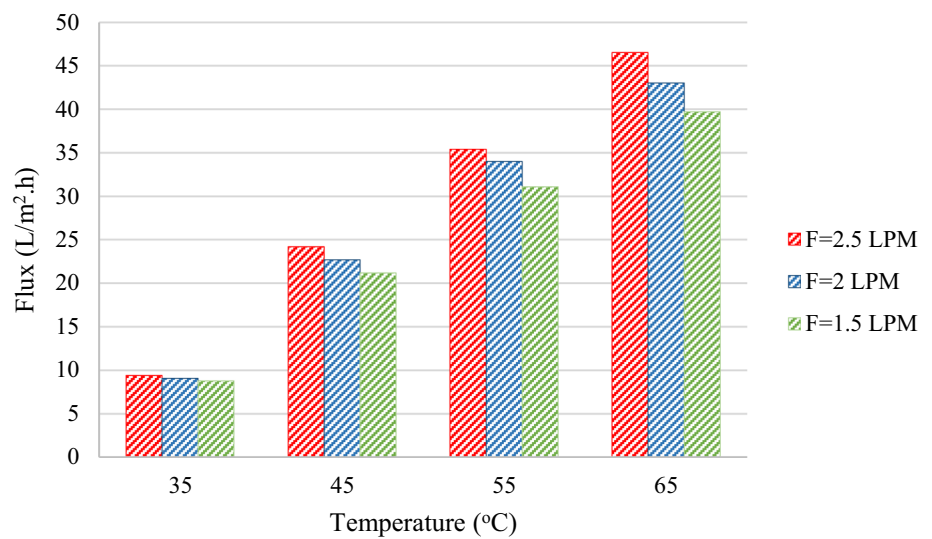

Fig. 11 Effect of temperature of the feed on flux of the permeate at different flow rates of the feed

results of permeate flux by varying the temperature from 35 to 65 °C, and flow rates of the feed from 1.5 LPM to 2.5 LPM are presented in Fig. 11 at a constant temperature of the permeate (20 °C).

As depicted in Fig. 11, elevating the flow rate of the feed from 1 LPM to 2.5 LPM results in an increase in the flux of the permeate from 35.2 to 46.5 kg/m² h, which shows about 32% improvement in the flux at 65 °C. However, at the temperatures of 35, 45 and 55 °C the flux was improved about 28%, with the same change in the flow rate of the feed. This phenomenon is related to the raising the Reynolds number of channel flow by raising the flow rate of the feed and consequently increasing the mass transfer coefficient in the membrane/bulk interface. Furthermore, the transfer resistances can be reduced by raising the Reynolds number, consequently leading to lessening the concentration and the temperature polarization effect.

In order to have a comparison between experimental data and correlated ones, the experiments were repeated at the flow rate of the feed of 1 LPM at different temperatures. As Fig. 12 indicates, raising the temperature of the feed results in a noteworthy raise in permeate flux because of the increases in vapor pressure. In other words, an exponential increase, from 7.88 to 35.2 L/m²h, can be seen in the permeate flux by raising the feed temperature from 35 to 65 °C, which the process can be correlated with an increase in vapor pressure.

Upon comparing the experimental data and theoretical results (as shown in Fig. 12), it can be observed that the error is less than 2%, suggesting that the model's predictions are highly reasonable.

Economic assessment

The economic assessment of industrial units is generally divided into two parts: initial investment costs (CAPEX) and operational costs (OPEX). Each of these two costs consists
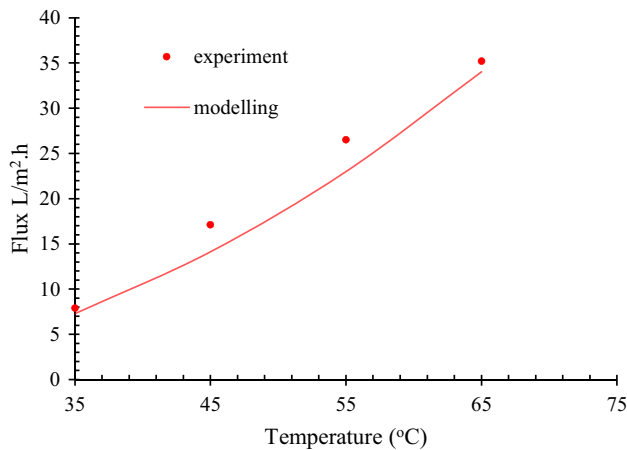
Fig. 12 The impact of the feed temperature on the permeate flux at flow rate of the feed of 1 LPM

of different sections and items, which will be discussed further. It should be mentioned that in this work, conventional cost estimation methods have been applied to calculate the expense of the membranes and process equipment.

The expense of the membrane comprises the price of the membrane module and the membrane itself, which is directly proportional to the membrane's active surface area used in the process. The construction and installation costs are related to the construction of buildings and structures required for the installation and operation of the equipment. The total electricity consumed cost during the construction of the unit, the expense of generators and the cost of energy consumed inside the site constitute the energy cost of the construction of the unit.

Piping costs include high-pressure pumps, process piping, pumps and transfer piping within the unit plant. Engineering costs also include the costs of contracts and personnel training. Indirect costs are usually considered as percentages of the total direct investment cost in economic estimates.

The operating costs are those costs incurred after the plant is in operation and during actual operations. These costs include energy costs (heating and electricity), replacement of membranes and other equipment, chemicals, labor and regular maintenance inspections. Most of the cost of the energy of water purification units is related to the consumption of the energy of the pumps. The high-pressure pumps applied in the NF process and pumps of other processes are among the major energy consumers in pressure-driven water treatment units.

The labor cost is another significant part of operating costs, which is related to the wages of employees and unit operators. The cost is determined by a percentage of the fixed expense. The cost of replacing and washing the membranes depends on the number of times of monthly washing and the lifetime of the membrane. Determining the membrane

washing times is not possible without conducting a practical pilot test in a long period of time, and in different units, it varies from several times a month to once every six months, and it is dependent on the type of feed and pre-treatment steps. To calculate the membrane washing costs, the washing times is determined based on the fouling data obtained from the laboratory setup and other similar industrial units. The membrane replacement time is also determined based on the recommended lifespan of the manufacturer and the information of similar industrial units. The repairment and replacement costs of the equipment, chemicals and side costs such as insurance and laboratory costs are among other items considered in this economical estimation.

NF process economic assessment

The detail of the Sethi and Wiesner (Sethi and Wiesner 2000; Hashemi et al. 2022) cost model is presented in Table 4, and the economic data required for the economic calculations of the nanofiltration process are given in Table 5.

In order to estimate and check the costs of the treatment unit, basic design was carried out for different input feed capacities. The type of treatment unit design has a significant effect on costs. In this case, designs were made to achieve a recovery rate of 70%. A summary of the design specifications of the nanofiltration unit can be seen in Table 6. These specifications as well as the information obtained from the experiments and similar units were used to estimate the costs.

The economic assessment of the nanofiltration process for the capacity of 2000 m^3/day was carried out using the Sethi and Wiesner model (Sethi and Wiesner 2000). The annual unit cost, which is calculated per m^3 of obtained water, represents the total of the yearly capital return and operating expenses. The annual return of capital is the amount of annual payment with a certain percentage of interest to compensate the initial investment cost during n years of the unit's life. The unit cost of water calculated for the nanofiltration process using the mentioned method is 0.63 ($/$m^3$).

In these calculations, the details of fixed costs were specified. In this method, the initial investment costs of a membrane water treatment unit consist of various components, like the price of membranes, pumps, tanks, pipes and connections, equipment installation and commissioning. Table 7 summarizes the fixed costs of the NF process.

Also, the operating costs of a water treatment unit in this model using NF process include energy costs, maintenance, membrane replacement costs, waste disposal costs and chemical costs which are listed in Table 8.

Moreover, to check the effect of the unit capacity on the output water expense, these calculations were repeated for other capacities. As it can be understood from Fig. 13, with the increase in the capacity of the process, makes the

Table 4 The details of the Sethi & Wiesner (Sethi & Wiesner 2000) cost model

Fixed cost ($)	
$K_{pv} = 5926.13 \times (A_m)^{0.42} \times CE$	Cost of pipes and valves (Kpv)
$K_{ic} = 1445.5 \times (A_m)^{0.66} \times CE$	Instrument and control costs (Kic)
$K_{tf} = 3047.21 \times (A_m)^{0.53} \times CE$	Cost of tanks (K_{tf})
$K_{mi} = 7865.02 \times (A_m)^{0.57} \times CE$	Miscellaneous cost (K_{mi})
$K_p = 622.59 \times (Q_f \times P)^{0.39} \times CE$	Pump cost (K_p)
$K_m = A_m \times c_m$	Membrane cost (K_m)
$K_{pv} = N \times c_{pv}$	Module cost (K_{pv})
$K_i = 0.25 \times (K_{pv} + K_{ic} + K_{tf} + K_p + K_p + K_m + K_{pv})$	Installation cost (K_i)
$C_c = K_{pv} + K_{ic} + K_{tf} + K_{mi} + K_p + K_m + K_{pv} + K_i$	Total fixed costs (C_c)
Operational cost ($/m^3$)	
$K_{rm} = \dfrac{a_m \times K_m}{Q \times f \times 24 \times 365}$	Membrane replacement cost (K_{rm})
$a_m = \dfrac{i}{(1+i)^{nm} - 1}$	
$K_{en} = \dfrac{Q_f \times P \times c_e}{\eta \times Q_f}$	Energy consumption cost (K_{en})
$K_{ch} = 0.0225 \times Q_p \times 24 \times 365$	Cost of chemicals used (K_{ch})
$K_{ma} = \dfrac{0.02 \times Cc}{Q_f \times f \times 24 \times 365}$	Maintenance cost (K_{ma})
$K_b = (1 - R) \times 0.066$	Cost of waste disposal (K_b)
$C_{O\&M} = K_{rm} + K_{en} + K_{ch} + K_{ma} + K_b$	Total operating cost ($C_{O\&M}$)

Table 5 Data and assumptions of the NF economic study

Availability factor (f)	0.9
Interest rate (i)	0.05
Plant life (n)	20
Membrane life (n)	5
Amortization factor (a)	$a = \dfrac{i(i+1)^n}{(i+1)^n - 1}$
Pump efficiency (η)	0.8
Specific cost	
Electricity cost (C_e)	0.13($/KW h)
Chemical cost (C_c)	0.066($/m^3$)
Membrane cost	60 ($/m^2$)
Labor cost (C_l)	0.03 ($/m^3$)

Table 6 The design specifications of the nanofiltration process

Feed flow rate	Pressure	Membrane active surface	Recovery ratio
83.3 m^3/h	9 bar	3427 cm^2	70%

Table 7 The fixed costs of the NF process

Cost of pipes and valves (K_{pv})	298,100 $
Instrument and control costs (K_{ic})	517,940 $
Cost of tanks (K_{tf})	376,960 $
Miscellaneous cost (K_{mi})	1,348,100 $
Pump cost (K_p)	80,331 $
Membrane & module cost (K_m)	237,690 $
Installation cost (K_i)	377,760 $
Total fixed costs (C_c)	3,236,900 $

According to Fig. 14, it can be understood that the effect of increasing the capacity on the initial investment is much more significant. This means that the annual return of capital compared to the annual operating costs constitutes a much larger component of the total annual cost in small units. This ratio decreases from 62% for the smallest unit to 51% for the largest unit.

DCMD process economic assessment

To assess the economic viability of the DCMD plant, it is necessary to calculate the water unit cost. The CAPEX involves direct and indirect capital cost. The direct cost is composed of civil work, pretreatment, pumps, membrane and heat exchanger, while the indirect cost is composed of insurance, freight and construction overhead. According to

process more economical. It can be seen that the effect of increasing the capacity in smaller units is very significant in such a way that by doubling the input flow of the process, therefore, the annual cost is reduced to $0.28. But this trend decreases in higher capacities and reaches $0.05 for doubling the capacity.

Table 8 The operating costs of the NF process

Membrane replacement cost	The cost of energy consumption	Cost of chemicals	maintenance cost	Cost of waste disposal	Total operating cost
0.059 $/m^3	0.0406 $/m^3	0.0318 $/m^3	0.0985 $/m^3	0.0132 $/m^3	0.2432 $/m^3

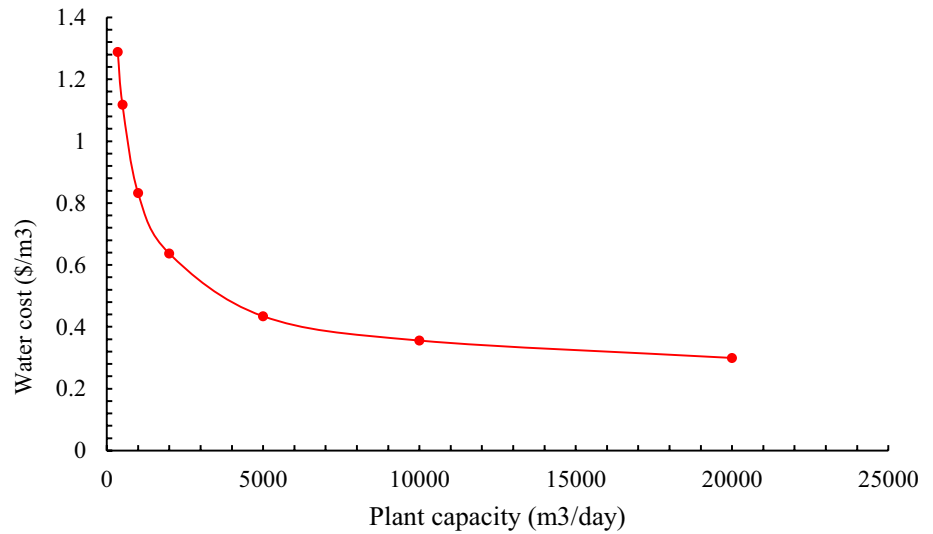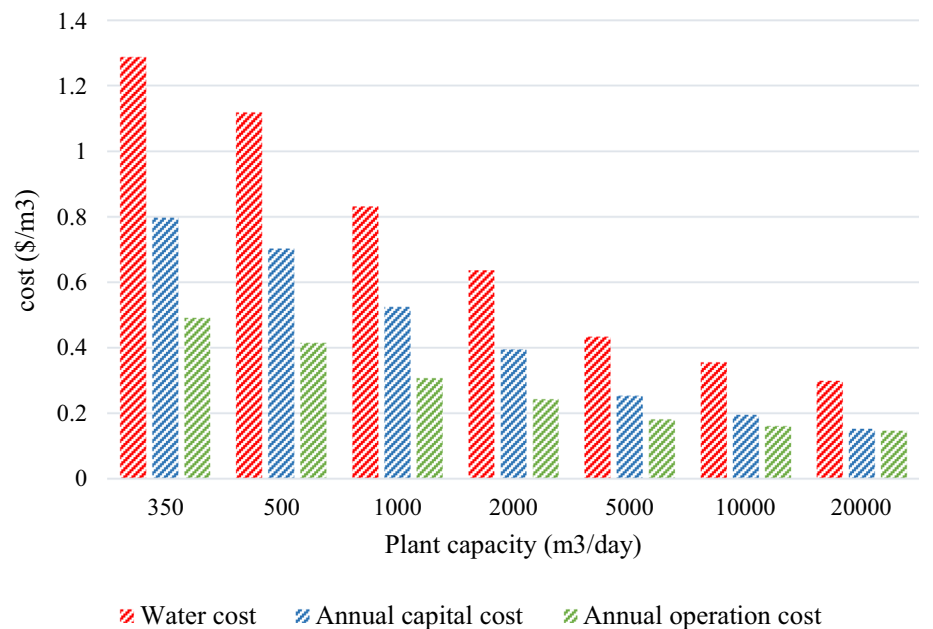**Fig. 13** The effect of nanofiltration unit capacity parameter on the price of the obtained water

Fig. 14 The effect of nanofiltration unit capacity on fixed and operating costs

literature, it was found that the indirect cost can be considered equal to 10% of the direct cost in the case of the DCMD plant (Tavakkoli et al. 2017). On the other hand, the OPEX consists of electrical energy, labor, maintenance, spares, chemicals, membrane replacement, brine disposal and steam.

In this work, the economic calculation was carried out based on the recent economic data (Sethi and Wiesner 2000) for a DCMD process (2000 m^3/day). The capital cost and operating cost equations as well as economic assumptions are presented in Tables 9 and 10, respectively.

The temperature difference (ΔT) effect on OPEX, CAPEX and water unit cost is investigated. In order to set

Table 9 The capital cost and operating cost equations

Capital cost
Civil work cost (\$) $= 1945(F)^{0.8}$
Cost of intake and pretreatment (\$) $= 658(F/DCMD\ recovery)^{0.8}$
Feed pumps cost (\$) $= 4.78 \times 10^{-6} (F/DCMD\ recovery)P$
Total cost of membrane (\$) $=$ (area of membrane) $\times$ (unit area cost of membrane)
Heat exchangers cost (\$) $=$ area of heat exchanger $\times$ unit area cost
Total costs of capital (\$) $=$ sum of all costs of above
Indirect costs of capital (\$) $= 0.1 \times$ total direct costs of capital
Total costs of capital (\$) $=$ direct costs $+$ indirect
Operating cost
Cost of membrane replacement (\$/year) $= 0.15 \times$ membrane costs
Cost of electricity (\$/year) $= \sum E \times c_e \times 24 \times f \times 365$
$\sum_i E = \dfrac{P_i \times 6.9 \times v_i}{\eta}$
Cost of chemical (\$/year) $= C_c \times f \times F \times 365$
Cost of steam (\$/year) $=$ (Required heat) $\times$ (heating value of fuel) $\times$ (price of fuel)
Cost of spares (\$/year) $= C_s \times f \times F \times 365$
Cost of labors (\$/year) $= C_l \times f \times F \times 365$
Cost of brine disposal (\$/year) $= C_b \times f \times F \times 365$
Total annual O&M cost (\$/year) $=$ sum of all above

Table 10 Data and assumptions of the DCMD economic study

Availability factor (f)	0.9
Interest rate (i)	0.05
Plant life (n)	20
Amortization factor (a)	$a = \dfrac{i(i+1)^n}{(i+1)^n - 1}$
Pump efficiency (η)	0.8
Electricity cost (C_e)	0.13(\$/KW h)
Chemical cost (C_c)	0.018(\$/m^3)
Membrane cost	90(\$/m^2)
Labor cost (C_l)	0.03(\$/m^3)
Brine disposal (C_b)	0.0015(\$/m^3)
Spares cost (C_s)	0.033(\$/m^3)
Steam heat exchanger cost	2000(\$/m^2)

the ΔT, a trade-off should be carried out because elevating the ΔT can enhance the permeate flux, so less membrane area is needed that can reduce the CAPEX; on the other hand, more heat energy is required at higher temperature differences which can increase the OPEX. Consequently, in order to minimize the water cost, an optimization has to be considered between the membrane and the heating costs by increasing the operating temperature differences between the two membrane sides of DCMD. Figure 15 illustrates that the minimum water cost is \$1.34/m^3, which is obtained when the plant operates at the temperature difference of 35 °C.

As DCMD should be a cost-competitive plant, a cost comparison is essential between the DCMD and other conventional technologies. The evaluated water cost in the case of MD using economic evaluation is \$1.34/m^3, while the water cost in the case of MED, MSF and RO is \$1.4/m^3, \$1/m^3 and \$0.5/m^3, respectively (Turchi et al. 2015). In addition to its competitive cost, it should be noted that the cost of the DCMD can be reduced further using available waste heat.

As the DCMD plant's capacity is a significant cost determinant, a broad spectrum is selected to distinctly observe the impact of scale-up on the cost of water per unit. Figure 16 shows the economic study of the DCMD plant for the capacity in the range of 2000–50,000 m^3/day.

The components of the total annual cost are shown in Fig. 17.

According to Fig. 17 it was found that the steam price is the main cost to supply the required thermal energy for heating the feed stream. It is evident that in order to generate the required steam in the DCMD plant, an available fuel should be used. The steam cost depends on two factors, the fuel cost and the heating value of the fuel. As a result, the selection of the appropriate fuel has a considerable effect on the unit water cost. For the purpose of comparison, the water unit cost was calculated for four different fuels, and the results are plotted in Fig. 18. According to the results, natural gas is the best fuel for the steam production in the DCMD plant that can reduce the water cost to about one quarter compared to gasoline.

The cost of the membrane is one of the effective parameters in the produced water cost using this process. This parameter has a direct impact on both initial investment costs and operational costs. Therefore, the produced MD process water cost is influenced by membrane expenses. As depicted in Fig. 19, the price of the obtained water increases with the

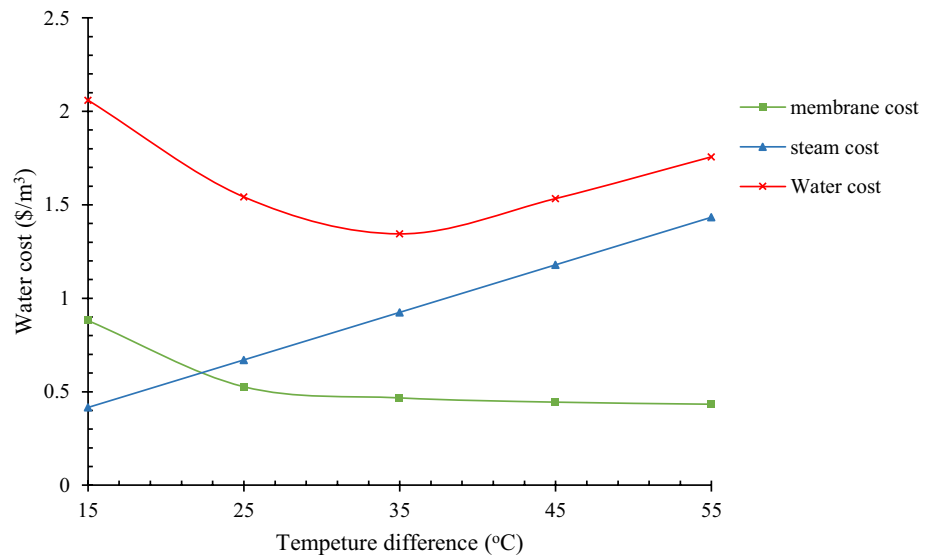**Fig. 15** Effects of the temperature difference (*ΔT*) on membrane, steam and water cost

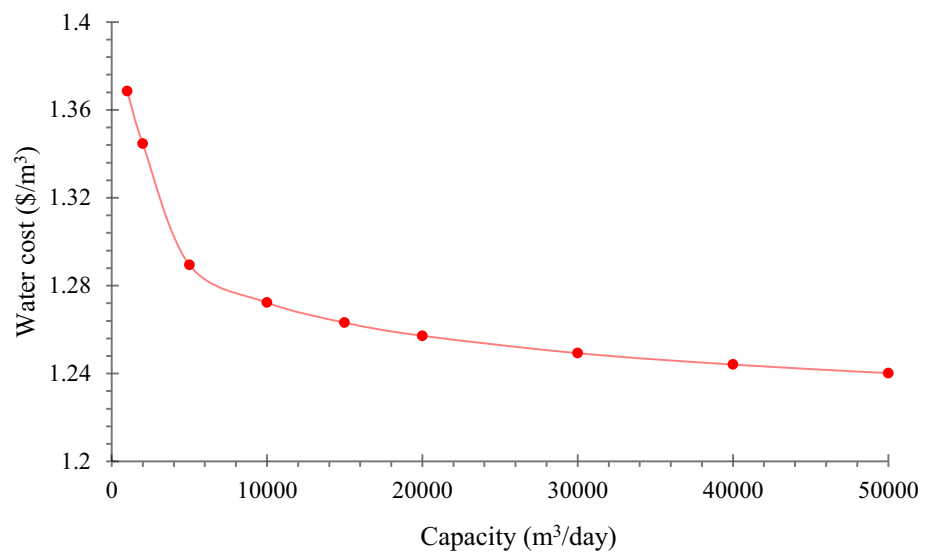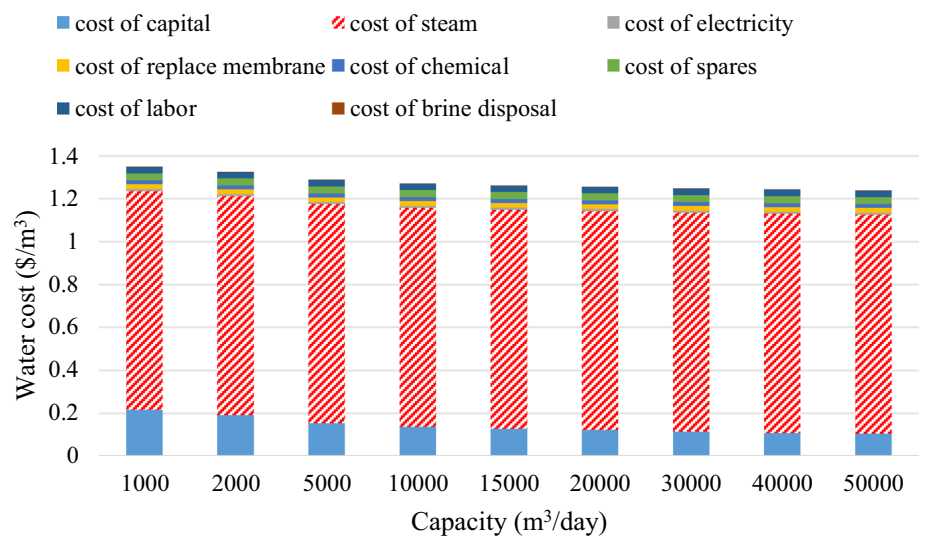**Fig. 16** Effect of plant capacity on water cost

Fig. 17 Total cost distribution over different annual cost components
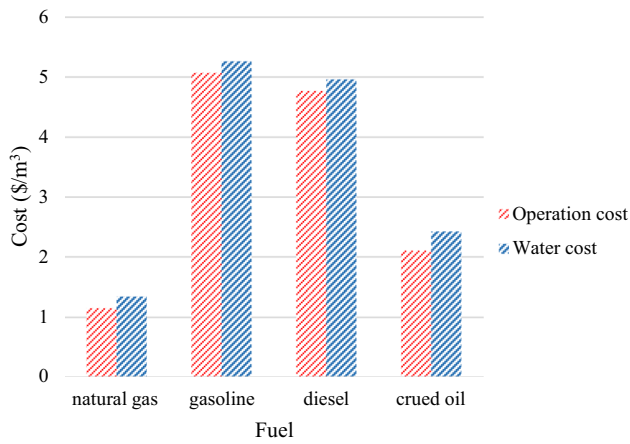
Fig. 18 The effect of different fuels on water unit cost

raise in the unit price of the applied membrane. Therefore, with the advancement of the applied membrane technology of the MD method, it is hoped that the price of membrane distillation membranes will decrease and of course this process will become more economical.

Nanofiltration and direct contact membrane distillation had different performances in improving the desired groundwater. So, the process of nanofiltration improves the water sample for agricultural purposes by reducing the TDS of the desired water to about 2000 ppm. The output water from the nanofiltration process is not suitable for drinking purposes. But direct contact membrane distillation process produces water with TDS = 18 ppm, providing very high-quality water. The water produced from MD process is not suitable for agricultural and drinking purposes neither. Nevertheless, the nanofiltration process permeate flux is higher than the DCMD process (46.5 and 65 L/m^2 h for the DCMD and nanofiltration processes, respectively).
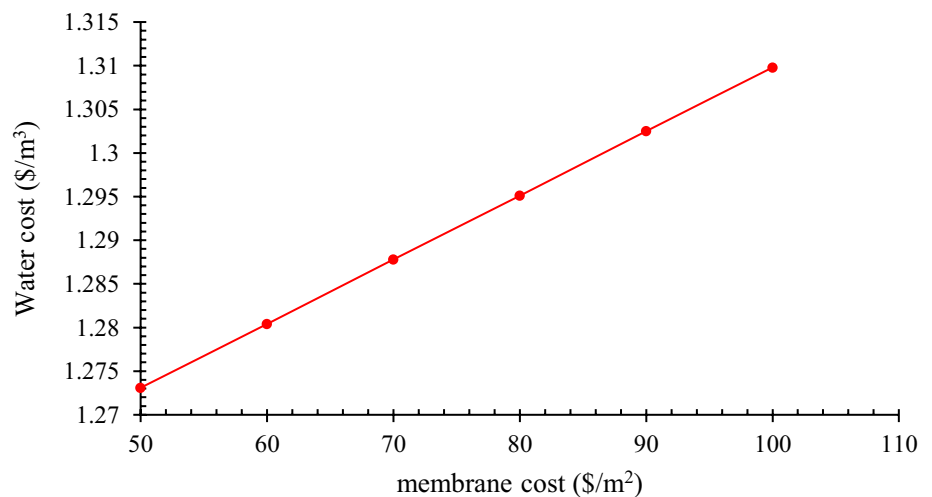
The economic analysis showed that the nanofiltration process has the lowest unit price of produced water compared to the DCMD process (1.34 and 0.9 \$/m^3 for DCMD and nanofiltration, respectively). The estimated fixed cost for the nanofiltration process is higher than the DCMD process, but the operating costs of the membrane distillation process are significantly higher than the nanofiltration process.

The most important reason for the increase in operating costs of membrane distillation is the high consumption of the energy to warm the saline water of the feed. As this parameter has the greatest impact on the costs of this system, the unit price of the membrane distillation process permeate water becomes much more suitable and competitive if other energy sources can be used.

According to the presented results, the price of the obtained water from the MD system is less sensitive to the increase in the unit capacity, while this parameter is more sensitive for the nanofiltration system, and with the increase in the unit capacity, the decrease in the price of water is more noticeable than in the MD process. The results show that the nanofiltration process has the ability to remove 50% of dissolved solids in the target water sample, which is suitable for agricultural purposes. However, the DCMD process has the ability to remove more than 99.9% of dissolved solids in the desired water sample, which is suitable in industrial applications due to its high purity.

Conclusions

So far, many studies have been conducted on MD or NF processes; nevertheless, no comprehensive study has been carried out to compare these two processes from the economic and process point of view. In this work, these two desalination processes were chosen to improve the quality

Fig. 19 The impact of membrane cost on the water production price in the DCMD method

of specific underground water with the aim of improving the quality for industrial purposes. According to the impact of various factors on the efficiency of these two processes, two parameters of temperature of the feed and the flow rate of the feed for MD process, and feed pressure and flow rate of the feed for NF process were evaluated. Then, using the obtained data, two processes were scaled up and evaluated according to the existing economic methods. Finally, two processes were compared with each other in terms of performance and economic efficiency. Due to the consumed energy price and the heating value on the total cost of the process, it was appropriately discussed economically. In this way, the performance of DCMD and NF using commercial polytetrafluoroethylene membrane was investigated, and the most critical variables were studied including flow rate of the feed and temperature of the feed. The unit cost of DCMD was calculated using experimental methods. The price of obtained water for a unit of 2000 cubic meters per day was 1.37 ($/m^3). By performing economic calculations in different capacities, it was observed that the process becomes more economical with increasing capacity. Finally, a predictive model is developed employing mathematical equations to solve for heat and mass transfer, concurrently. Comparing the experimental data and the results obtained from the MD process correlation using equations governing heat transfer and mass transfer, showed that the error of the performed modeling was less than 3%, which shows that the prediction of the model is quite reasonable and can be used in different operating conditions. It should be mentioned that even though the cost of the water production using DCMD is slightly higher than RO but quite comparable with other conventional desalination methods. This may be due to the fact that this technology is not developed very well in comparison with other well-known desalination methods, industrially; nevertheless, the research trend reveals that it has a great potential to be a bright technology in the field of water desalination. It must be mentioned that the cost of water can be even lower by reducing the steam-generating costs using inexpensive fuels or renewable energy in DCMD. It would be more feasible, if the water production plant had access to excess low-pressure vapor in industry plants like refineries, power plants, etc. It is suggested that, in the continuation of this work, the performance of the NF-DCMD hybrid method for the treatment of different waters and its economic evaluation is carried out. In addition to evaluating the performance of the NF-DCMD hybrid method for treating different waters and conducting its economic assessment, future work will consider incorporating economic assessments specifically for feedwaters with higher salinity levels, such as brackish water with TDS around 12,000 ppm. This inclusion aims to assess the cost-effectiveness and feasibility of implementing the NF-DCMD hybrid method in scenarios involving more saline feeds, aligning with the intended application of MD processes for handling extremely saline waters.

Declarations

References

Ahmed S, Bashir S, Ali M (2019) Factors causing water scarcity in washuk district Balochistan. Balochistan Rev 40(1).

Alqaydi M, Mavukkandy MO, Mustafa I, Alnuaimi A, Arafat HA, Almarzooqi F (2022) Activated carbon as a photothermal absorber in PVDF membranes for solar driven air-gap membrane distillation. Desalination 541:116031

Anbazhagan L, Sudhanya P, Jansi R (2023) Characteristics analysis of different photonic crystal fiber lattice structures. J Opt Photon Res.

Aydın AB, Tuna MC (2018) Research on the importance of groundwater. ISS2018, 8.

Bouchrit R, Boubakri A, Hafiane A, Bouguecha SA-T (2015) Direct contact membrane distillation: capability to treat hyper-saline solution. Desalination 376:117–129

Chen Y, Zhu H, Tian J, Fu Y, Tang Z, Wang N (2017) Convective heat transfer characteristics in the laminar and transition region of molten salt in concentric tube. Appl Therm Eng 117:682–688

Chen H, Wu S-L, Wang H-L, Wu Q-Y, Yang H-C (2021) Photothermal devices for sustainable uses beyond desalination. Adv Energy Sustain Res 2(3):2000056

Curcio E, Drioli E (2005) Membrane distillation and related operations—a review. Sep Purif Rev 34(1):35–86

Elhenawy Y, Moustafa G, Attia AM, Mansi A, Majozi T, Bassyouni M (2022) Performance enhancement of a hybrid multi effect evaporation/membrane distillation system driven by solar energy for desalination. J Environ Chem Eng 10(6):108855

Generous MM, Qasem NA, Zubair SM (2021) Entropy generation analysis of electrodialysis desalination using multi-component groundwater. Desalination 500:114858

Guo X-S, Nian T-K, Gu Z-D, Li D-Y, Fan N, Zheng D-F (2021) Evaluation methodology of laminar-turbulent flow state for fluidized material with special reference to submarine landslide. J Waterw Port Coast Ocean Eng 147(1):04020048

Halder A, Tanshen MR, Hossain MA, Akter MS, Sikdar MA (2024) Tailored dispersion and nonlinear effects in flint glass honeycomb PCF for optical communication. J Opt Photon Res 1(1).

Hamta A, Dehghani MR (2017) Application of polyethylene glycol based aqueous two-phase systems for extraction of heavy metals. J Mol Liq 231:20–24

Hamta A, Dehghani MR, Gholami M (2017) Novel experimental data on aqueous two–phase system containing PEG–6000 and Na2CO3 at T=(293.15, 303.15 and 313.15) K. J Mol Liq 241:144–149

Hashemi F, Hashemi H, Abbasi A, Schreiber ME (2022) Life cycle and economic assessments of petroleum refineries wastewater recycling using membrane, resin and on site disinfection (UF-IXMB-MOX) processes. Process Saf Environ Prot 162:419–425

Ismail M, Mohamed A, Poggio D, Walker M, Pourkashanian M (2022) Modelling mass transport within the membrane of direct contact membrane distillation modules used for desalination and wastewater treatment: Scrutinising assumptions. J Water Process Eng 45:102460

Jawad J, Hawari AH, Zaidi SJ (2021) Artificial neural network modeling of wastewater treatment and desalination using membrane processes: A review. Chem Eng J 419:129540

König K (2023) Multimodal multiphoton tomography with a compact femtosecond fiber laser. J Opt Photon Res.

Kukučka M, Kukučka Stojanović N (2022) Intrinsic dependence of groundwater cation hydraulic and concentration features on negatively charged thin composite nanofiltration membrane rejection and permeation behavior. Membranes 12(1):79

Lawson KW, Lloyd DR (1996) Membrane distillation. I. Module design and performance evaluation using vacuum membrane distillation. J Membr Sci 120(1):111–121

Lee T, Min C, Naidu G, Huang Y, Shon HK, Kim S-H (2022) Optimizing the performance of sweeping gas membrane distillation for treating naturally heated saline groundwater. Desalination 532:115736

Li J, Zhang C, Wang Z, Bai Z, Kong X (2022) Salinity gradient energy harvested from thermal desalination for power production by reverse electrodialysis. Energy Convers Manage 252:115043

Luo X, Wen X, Li Y, Li Q (2023) Pruning method for dendritic neuron model based on dendrite layer significance constraints. CAAI Trans Intell Technol 8(2):308–318

Mahmood T, Rehman U, ur Ali Z, Haleemzai I (2023) Analysis of TOPSIS techniques based on bipolar complex fuzzy N-soft setting and their applications in decision-making problems. CAAI Trans Intell Technol 8(2):478–499

Manawi YM, Khraisheh M, Fard AK, Benyahia F, Adham S (2014) Effect of operational parameters on distillate flux in direct contact membrane distillation (DCMD): comparison between experimental and model predicted performance. Desalination 336:110–120

Meyer JP, Everts M, Coetzee N, Grote K, Steyn M (2019) Heat transfer coefficients of laminar, transitional, quasi-turbulent and turbulent flow in circular tubes. Int Commun Heat Mass Transfer 105:84–106

Nthunya LN, Bopape MF, Mahlangu OT, Mamba BB, Van der Bruggen B, Quist-Jensen CA, Richards H (2022) Fouling, performance and cost analysis of membrane-based water desalination technologies: a critical review. J Environ Manage 301:113922

Oré D, Pretell V, Pilco A (2022) Design of an autonomous photovoltaic system for desalination of groundwater by electrodialysis. J Phys Confer Series. IOP Publishing, UK.

Patel SK, Ritt CL, Deshmukh A, Wang Z, Qin M, Epsztein R, Elimelech M (2020) The relative insignificance of advanced materials in enhancing the energy efficiency of desalination technologies. Energy Environ Sci 13(6):1694–1710

Rosentreter H, Walther M, Lerch A (2021) Partial desalination of saline groundwater: comparison of nanofiltration, reverse osmosis and membrane capacitive deionisation. Membranes 11(2):126

Santos PG, Scherer CM, Fisch AG, Rodrigues MAS (2021) Water–energy nexus in membrane distillation: Process design for enhanced thermal efficiency. Ind Eng Chem Res 60(11):4430–4439

Sethi S, Wiesner MR (2000) Simulated cost comparisons of hollow-fiber and integrated nanofiltration configurations. Water Res 34(9):2589–2597

Shirzadi M, Li Z, Yoshioka T, Matsuyama H, Fukasawa T, Fukui K, Ishigami T (2022) CFD model development and experimental measurements for ammonia-water separation using a vacuum membrane distillation module. Ind Eng Chem Res 61(21):7381–7396

Srivastava A, Aghilesh K, Nair A, Ram S, Agarwal S, Ali J, Singh R, Garg MC (2021) Response surface methodology and artificial neural network modelling for the performance evaluation of pilot-scale hybrid nanofiltration (NF) & reverse osmosis (RO) membrane system for the treatment of brackish ground water. J Environ Manage 278:111497

Stein S, Sivan O, Yechieli Y, Kasher R (2021) Redox condition of saline groundwater from coastal aquifers influences reverse osmosis desalination process. Water Res 188:116508

Subramani A, Jacangelo JG (2015) Emerging desalination technologies for water treatment: a critical review. Water Res 75:164–187

Subramanian N, Qamar A, Alsaadi A, Gallo A Jr, Ridwan MG, Lee J-G, Pillai S, Arunachalam S, Anjum D, Sharipov F (2019) Evaluating the potential of superhydrophobic nanoporous alumina membranes for direct contact membrane distillation. J Colloid Interface Sci 533:723–732

Tavakkoli S, Lokare OR, Vidic RD, Khanna V (2017) A techno-economic assessment of membrane distillation for treatment of Marcellus shale produced water. Desalination 416:24–34

Tawalbeh M, Al Mojjly A, Al-Othman A, Hilal N (2018) Membrane separation as a pre-treatment process for oily saline water. Desalination 447:182–202

Tayefeh M (2022) An innovative rearrangement and comprehensive comparison of the combination of compressed air energy storage (CAES) with multi stage flash (MSF) desalination and multi effect distillation (MED) systems. J Energy Storage 52:105025

Turchi CS, Akar S, Cath T, Vanneste J, Geza M (2015) Use of low-temperature geothermal energy for desalination in the Western United States, National Renewable Energy Lab.(NREL), Golden, CO (United States).

Usman HS, Touati K, Rahaman MS (2021) An economic evaluation of renewable energy-powered membrane distillation for desalination of brackish water. Renew Energy 169:1294–1304

Yang S, Jasim SA, Bokov D, Chupradit S, Nakhjiri AT, El-Shafay A (2022) Membrane distillation technology for molecular separation: a review on the fouling, wetting and transport phenomena. J Mol Liq 349:118115

Zhao G, Zhang Y, Ge M, Yu M (2023) Bilateral U-Net semantic segmentation with spatial attention mechanism. CAAI Trans Intell Technol 8(2):297–307

Authors and Affiliations

**Noureddine Elboughdiri[1,2] · Renzun Cosma[3] · Abdelfattah Amari[4] · Velibor Spalevic[5,6] · Branislav Dudic[7,8] ·
Goran Skataric[9,10]**

✉ Branislav Dudic
branislav.dudic@fm.uniba.sk

Noureddine Elboughdiri
ghilaninouri@yahoo.fr

Renzun Cosma
renzuncosma@gmail.com

Abdelfattah Amari
abdelfattah.amari@enig.rnu.tn

Velibor Spalevic
velibor.spalevic@gmail.com

[1] Chemical Engineering Department, College of Engineering, University of Ha'il, P.O. Box 2440, Ha'il 81441, Saudi Arabia

[2] Chemical Engineering Department, Modelling Analysis and Control of Systems, National School of Engineering Gabes, University of Gabes, 6029 Gabes, Tunisia

[3] Department of Industrial Engineering, Antonio Ruiz de Montoya University, Lima, Peru

[4] Department of Chemical Engineering, College of Engineering, King Khalid University, 61411 Abha, Kingdom of Saudi Arabia

[5] Biotechnical Faculty, University of Montenegro, 81000 Podgorica, Montenegro

[6] Faculty of Philosophy, Geography, University of Montenegro, 81400 Niksic, Montenegro

[7] Faculty of Management, Comenius University Bratislava, 81499 Bratislava, Slovakia

[8] Faculty of Economics and Engineering Management, University Business Academy, 21000 Novi Sad, Serbia

[9] Management, Maritime Faculty, University of Montenegro, 85331 Kotor, Montenegro

[10] Marketing, Faculty of Sports and Physical Education, University of Montenegro, 81400 Niksic, Montenegro